

Spin Splitting Induced Photogalvanic Effect in Quantum Wells

L.E. Golub*

A.F. Ioffe Physico-Technical Institute, Russian Academy of Sciences, 194021 St. Petersburg, Russia

A theory of the circular photogalvanic effect caused by spin splitting in quantum wells is developed. Direct interband transitions between the hole and electron size-quantized subbands are considered. The photocurrent excitation spectrum is shown to depend strongly on the form of the spin-orbit interaction. In the case of structure inversion asymmetry induced (Rashba) spin-splitting, the current is a linear function of light frequency near the absorption edge, and for the higher excitation energy the spectrum changes its sign and has a minimum. In contrast, when the bulk inversion asymmetry (Dresselhaus splitting) dominates, the photocurrent edge behavior is parabolic, and then the spectrum is sign-constant and has a maximum.

PACS numbers: 72.40.+w, 72.20.My, 72.25.Rb, 72.25.-b, 73.63.Hs

I. INTRODUCTION

Spin properties of carriers attract great attention in recent years due to rapidly developed spintronics dealing with manipulation of spin in electronic devices.¹ The first idea has been put forward by Datta and Das, who proposed a spin field-effect transistor.² Its work is based on a change of the Rashba field in semiconductor heterostructures, caused by structure inversion asymmetry (SIA).

The promising materials for spintronics are III-V semiconductor quantum wells (QWs) whose spin properties are well documented and can be controlled by advanced technology. However, in addition to the Rashba spin-orbit interaction, another effective magnetic field acts on carriers in zinc-blende heterostructures. This is the so-called Dresselhaus field caused by bulk inversion asymmetry (BIA).³

Both BIA and SIA give rise to many spin-dependent phenomena in QWs, such as an existence of beats in the Shubnikov-de Haas oscillations,⁴ spin relaxation,⁵ splitting in polarized Raman scattering spectra,⁶ and positive anomalous magnetoresistance.⁷ Spin splittings and relaxation times have been extracted from these experiments. However, in [001] QWs, the BIA and SIA spin-orbit interactions result in the same dependences of spin splittings and spin relaxation times on the wave vector. Therefore it is impossible to determine the nature for the spin splitting. Only in the simultaneous presence of both BIA and SIA of comparable strengths, one can observe new effects, see Ref. 8 and references therein. However the latter situation is rare in real systems because it requires a special structure design.

In this work, the other spin-dependent phenomenon is investigated which is essentially different from the mentioned above. This is the circular photogalvanic effect which is a conversion of photon angular momentum into a directed motion of charge carriers. This leads to an appearance of electric current under absorption of a circularly-polarized light.⁹ The photocurrent reverses its direction under inversion of the light helicity. Microscopically, the circular photocurrent appears owing to a cou-

pling between orbital and spin degrees of freedom. In semiconductors the coupling is a consequence of the spin-orbit interaction. In two-dimensional systems, the circular photogalvanic effect can be caused by both Rashba and Dresselhaus effective magnetic fields. In this paper we show that SIA and BIA result in experimentally distinguishable photocurrents.

Recently started activity on circular photogalvanics in QWs attracted big attention.^{10,11} The photocurrents induced by both BIA and SIA have been investigated. The circular photocurrent has been mostly studied under *intra*band optical transitions induced by infrared or far-infrared excitations. However it is important to extend the studies on the optical range where the effect is expected to be much stronger. In this case, the photocurrent appears due to *inter*band transitions.

In the present work, the theory of the interband circular photogalvanic effect in QWs is developed, and the photocurrent spectra are calculated.

II. THEORY

Spin splittings of electron or hole subbands give rise to the circular photogalvanic effect. In order to obtain non-zero photocurrent, it is enough to include spin-orbit interaction for only one kind of carriers. Here we take into account spin-orbit splitting in the conduction band. In QWs, the spin-orbit interaction is described by the linear in the wave vector Hamiltonian

$$H(\mathbf{k}) = \beta_{il} \sigma_i k_l, \quad (1)$$

where σ_i are the Pauli matrices.

Tensor β is determined by the symmetry of the QW. As mentioned in Introduction, in structures with a zinc-blende lattice, there is a contribution due to BIA known as the Dresselhaus term. For [001] QWs, it has two non-zero components, namely

$$\beta_{xx} = -\beta_{yy} \equiv \beta_{\text{BIA}}, \quad (2)$$

where $x||[100]$, $y||[010]$, and the z -axis coincides with the growth direction.

SIA appears due to inequivalence of the right and left interfaces of the QW, electric fields applied along z direction, etc. It leads to an additional contribution to the spin-orbit Hamiltonian, the so-called Rashba term:

$$\beta_{xy} = -\beta_{yx} \equiv \beta_{\text{SIA}}. \quad (3)$$

In the presence of the spin-orbit interaction (1), the two electron states with a given wave vector \mathbf{k} have a splitting $\Delta = 2\sqrt{(\beta_{xi}k_i)^2 + (\beta_{yi}k_i)^2}$. We denote these states by the index $m = \pm$. Their envelope functions in size-quantized subbands can be chosen in the form

$$|m\rangle = \exp(i\mathbf{k} \cdot \boldsymbol{\rho}) \varphi(z) \left[\frac{m}{\sqrt{2}} \exp(-i\Phi_{\mathbf{k}}) \uparrow + \frac{1}{\sqrt{2}} \downarrow \right], \quad (4)$$

where the phase $\Phi_{\mathbf{k}}$ is given by

$$\tan \Phi_{\mathbf{k}} = \frac{\beta_{xi}k_i}{\beta_{yi}k_i},$$

\uparrow and \downarrow are the spin-up and spin-down states, and $\boldsymbol{\rho}$ is the electron position in the plane of QW. For odd (even) subbands of size-quantization, $\varphi(-z) = \pm\varphi(z)$, respectively.

The two hole states in the same subband and with the same \mathbf{k} are assumed to be degenerate. We denote their dispersion, calculated in the spherical approximation, as $E_h(k)$. The states can be chosen as symmetrical (s) and antisymmetrical (a) in relation to the mirror reflection in the plane located in the middle of the QW. The corresponding wave functions have the form¹²

$$\begin{aligned} |s\rangle &= \exp(i\mathbf{k} \cdot \boldsymbol{\rho}) \quad (5) \\ &\times N \left\{ - \left[u_{3/2} + \sqrt{3}W_+ \exp(2i\phi_{\mathbf{k}})u_{-1/2} \right] C(z) \right. \\ &\left. + i\zeta \left[\exp(3i\phi_{\mathbf{k}})u_{-3/2} + \sqrt{3}W_- \exp(i\phi_{\mathbf{k}})u_{1/2} \right] S(z) \right\}, \end{aligned}$$

and $|a\rangle$ can be obtained from $|s\rangle$ by applying the operations of time- and space-inversion. Here $u_{\pm 3/2}$, $u_{\pm 1/2}$ are the Bloch functions at the top of the valence band, C and S are, respectively, even and odd functions of coordinate z ,¹³ and $\phi_{\mathbf{k}}$ is the angle between $[100]$ and \mathbf{k} :

$$\tan \phi_{\mathbf{k}} = k_y/k_x.$$

Let us now consider optical excitation of a QW by circularly-polarized light (see Fig. 1). Here we investigate the photocurrent arising due to asymmetry of the carrier distribution in \mathbf{k} -space at the moment of creation. It is different from another photocurrent caused by carrier momentum re-distribution during the process of spin relaxation. The latter, so-called spin-galvanic effect, was considered in Refs. 14 and 11. These two photocurrents can be separated in the time-resolved experiments: after switching-off the light source, the former decays with the momentum relaxation time while the latter disappears within the spin relaxation time.

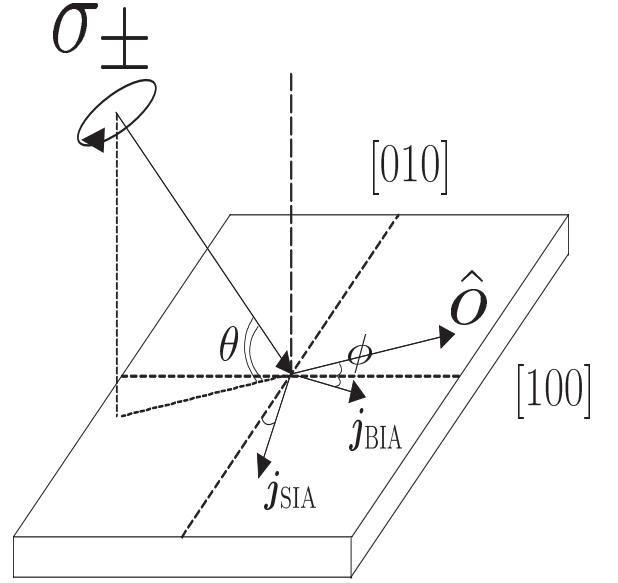


FIG. 1: SIA- and BIA-induced photocurrents appearing under oblique incidence of circularly-polarized light.

The electric current is expressed in terms of the velocity operators and spin density matrices for electrons and holes as follows

$$\mathbf{j} = e \sum_{\mathbf{k}} \text{Tr} \left[\mathbf{v}^{(e)}(\mathbf{k}) \rho^{(e)}(\mathbf{k}) - \mathbf{v}^{(h)}(\mathbf{k}) \rho^{(h)}(\mathbf{k}) \right], \quad (6)$$

where e is the electron charge.

The velocity matrix elements calculated on the wave functions (4), (5) taking into account the spin-orbit corrections (1), are given by

$$\begin{aligned} (v_i^{(e)})_{mm'} &= \left[\frac{\hbar k_i}{m_e} + \frac{m}{\hbar} (\beta_{xi} \cos \Phi_{\mathbf{k}} + \beta_{yi} \sin \Phi_{\mathbf{k}}) \right] \delta_{mm'} \\ &+ \frac{im}{\hbar} (\beta_{yi} \cos \Phi_{\mathbf{k}} - \beta_{xi} \sin \Phi_{\mathbf{k}}) (1 - \delta_{mm'}), \\ v_i^{(h)} &= \frac{k_i}{k} v_h(k), \quad v_h(k) = \frac{1}{\hbar} \frac{dE_h(k)}{dk}, \quad (7) \end{aligned}$$

where m_e is the electron effective mass.

Density-matrix equations taking into account both direct optical transitions and elastic scattering give the following expressions for linear in the light intensity values entering into Eq.(6)

$$\begin{aligned} \rho_{nn'}^{(e,h)} &= \pm \frac{\pi}{\hbar} \tau_{e,h} \sum_{\bar{n}} M_{n\bar{n}} M_{\bar{n}n'} \left[\delta(E_n + E_{\bar{n}} - \hbar\omega) \right. \\ &\left. + \delta(E_{n'} + E_{\bar{n}} - \hbar\omega) \right]. \quad (8) \end{aligned}$$

Here τ_e and τ_h are the relaxation times of electrons and holes (here we assume isotropic scattering), $\hbar\omega$ is the photon energy, $M_{n\bar{n}}(\mathbf{k})$ is the matrix element of the direct optical transition between the subbands n and \bar{n} , and the energy dispersions $E_{e,h}(\mathbf{k})$ are reckoned inside the bands.

Calculations show that all odd harmonics of $\rho^{(e,h)}(\mathbf{k})$ entering into (6) are proportional to the following part of

the sum

$$\begin{aligned} \sum_{l=s,a} M_{mi} M_{lm'} &\propto P_{circ} \left(\frac{epA_0}{m_0c} \right)^2 \sin \theta (NQ_{\pm})^2 m \quad (9) \\ &\times \{ \delta_{mm'} [W_{\pm} \cos(\Phi_{\mathbf{k}} - 2\phi_{\mathbf{k}} + \phi) + W_{\pm}^2 \cos(\Phi_{\mathbf{k}} - \phi)] \\ &+ i(1 - \delta_{mm'}) \\ &\times [W_{\pm} \sin(\Phi_{\mathbf{k}} - 2\phi_{\mathbf{k}} + \phi) + W_{\pm}^2 \sin(\Phi_{\mathbf{k}} - \phi)] \}. \end{aligned}$$

Here P_{circ} is the circular polarization degree, θ and ϕ are the spherical angles of the light polarization vector (see Fig. 1), p is the interband momentum matrix element, A_0 is the light wave amplitude, m_0 is the free electron mass, and

$$Q_+ = \int_{-\infty}^{\infty} dz \varphi(z) C(z), \quad Q_- = \zeta \int_{-\infty}^{\infty} dz \varphi(z) S(z). \quad (10)$$

The upper (lower) sign in Eq. (9) corresponds to excitation into the odd (even) electron subbands.¹³

The characteristic spin splittings are usually very small, therefore we consider a linear in β regime. In this approximation, SIA and BIA give independent contributions into the photocurrent

$$\mathbf{j}(\omega) = \mathbf{j}_{SIA}(\omega) + \mathbf{j}_{BIA}(\omega), \quad (11)$$

where \mathbf{j}_{SIA} and \mathbf{j}_{BIA} are linear in β_{SIA} and β_{BIA} , respectively. Assuming the splitting $\Delta \rightarrow 0$ and calculating the reduced density of states, we obtain from Eqs. (6) - (10) the expressions for the interband circular photocurrents:

$$j_i(\omega) = -\beta_{li} \hat{o}_l P_{circ} \left(\frac{epA_0}{m_0 \hbar c} \right)^2 \frac{e}{\hbar} G(k_{\omega}). \quad (12)$$

Here $i, l = x, y$, and \hat{o} is a projection of the unit vector along the light propagation direction on the QW plane (see Fig. 1). The wave vector of the direct optical transition, k_{ω} , satisfies the energy conservation law

$$E_e(k_{\omega}) + E_h(k_{\omega}) = \hbar\omega - E_g, \quad (13)$$

where $E_e(k)$ is the parabolic electron dispersion without spin-orbit corrections. We study the effects linear in β , therefore Eq. (12) is valid at $\hbar\omega - E_g^{QW} \gg \beta k_{\omega}$, where $E_g^{QW} = E_g + E_{e1}(0) + E_{h1}(0)$ is the fundamental energy gap corrected for the energies of size-quantization. However for real systems, the theory is valid even near the absorption edge.

The frequency dependence of the photocurrent is given by the function $G(k)$

$$G(k) = \frac{k}{v(k)} \frac{d}{dk} \left[\frac{F(k)u(k)}{v(k)} \right] - \frac{F(k)}{v(k)} \left[2 - \frac{u(k)}{v(k)} \right], \quad (14)$$

where

$$\begin{aligned} F(k) &= k [N(k)Q_{\pm}(k)W_{\pm}(k)]^2 \tau_e(k), \quad (15) \\ v(k) &= \frac{\hbar k}{m_e} + v_h(k), \quad u(k) = \left[\frac{\hbar k}{m_e} + v_h(k) \frac{\tau_h(k)}{\tau_e(k)} \right] \xi(k). \end{aligned}$$

The first term in Eq. (14) appears because the direct transitions to the upper (lower) spin branch take place at a wave vector slightly smaller (larger) than k_{ω} , and the second term occurs because the two electron spin states with the same \mathbf{k} have different velocities.

The factor $\xi(k)$ depends on the form of a spin-orbit interaction. It follows from Eqs. (2), (3) that, for the BIA-induced spin-orbit interaction, $\Phi_{\mathbf{k}} = -\phi_{\mathbf{k}}$, while, for SIA-dominance, $\Phi_{\mathbf{k}} = \phi_{\mathbf{k}} - \pi/2$. Therefore one has

$$\xi_{BIA} = 1, \quad \xi_{SIA} = 1 - 1/W_{\pm}(k). \quad (16)$$

The difference appears because in the BIA-case the terms with W_{\pm} in Eq. (9) are the third harmonics of $\phi_{\mathbf{k}}$ and, hence, do not contribute to the current. This means that BIA and SIA create different current distributions of optically-generated electrons.

This difference gives rise to non-equal frequency dependences of the photocurrent. It is dramatic at the absorption edge, when $\hbar\omega \geq E_g^{QW}$. For the ground hole subband $W_+(k) \sim k^2$, and hence

$$j_{BIA} \sim (\hbar\omega - E_g^{QW})^2, \quad j_{SIA} \sim \hbar\omega - E_g^{QW}. \quad (17)$$

This conclusion opens a possibility to distinguish experimentally which kind of asymmetry, BIA or SIA, is dominant in the structure under study. This could be done by studying the power, quadratic or linear, in the dependence of the circular photocurrent on the light frequency near the absorption edge. At higher photon energies, the spectra are also different due to k -dependence of the functions W_{\pm} [see Eq. (16)].

III. RESULTS AND DISCUSSION

Eqs. (11 - 16) describe the contributions to the circular photocurrent due to interband optical transitions. It is seen that the symmetry of the system determines the direction of the current. Indeed, according to Eq. (12), $j_i(\omega) \propto \beta_{li} \hat{o}_l$, i.e. (i) the current appears only under oblique light incidence and (ii) for SIA the current \mathbf{j} is perpendicular to \hat{o} , while for BIA the angle between \mathbf{j} and \hat{o} is twice larger than the angle between the axis [100] and \hat{o} , see Fig. 1.

The spectrum of the photocurrent is determined by the function $G(k_{\omega})$. Fig. 2 presents the partial contributions to this function for both SIA and BIA calculated for a 100-Å wide QW with infinitely-high barriers. The interband transitions between the $h1$, $h2$, $l1$ and $h3$ hole subbands and the ground electron subband, $e1$, are taken into account. The effective masses of the electron, heavy- and light-holes are chosen to correspond to GaAs: $m_e = 0.067m_0$, $m_{hh} = 0.51m_0$, $m_{lh} = 0.082m_0$. The momentum relaxation times are assumed to be related by $\tau_h = 2\tau_e$ and independent of the carrier energies.¹⁵

The edge behavior of the photocurrent is due to the $h1 \rightarrow e1$ transitions. One can see the linear and quadratic raising of the current near the absorption edge

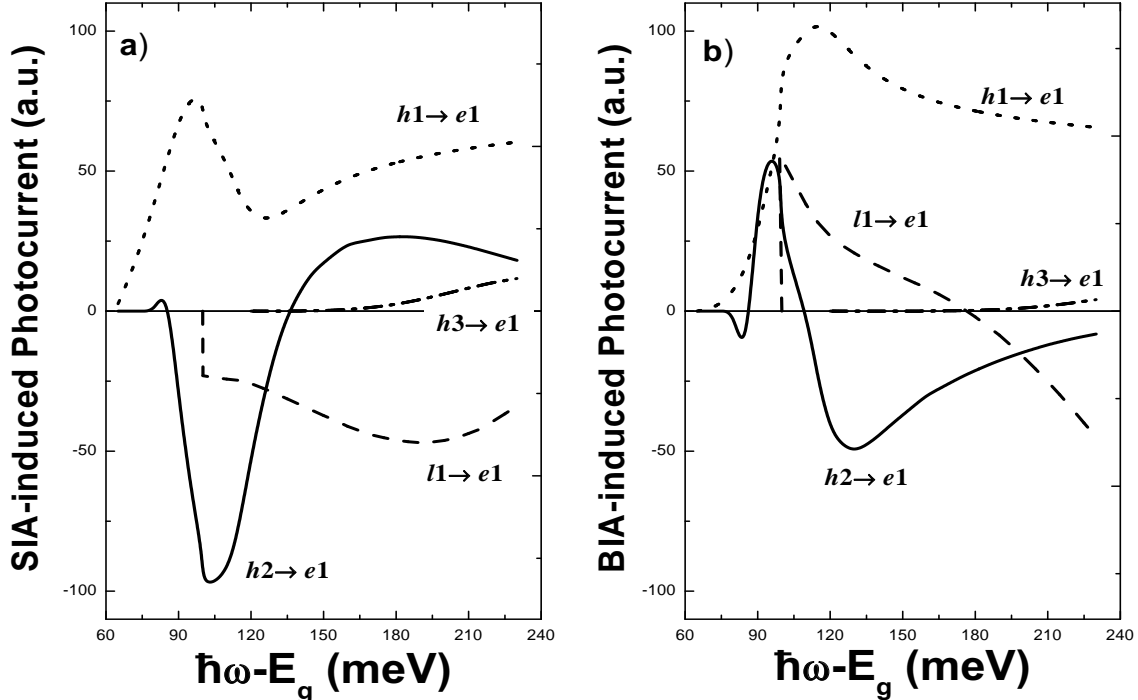


FIG. 2: Partial contributions to the circular photocurrent for direct interband transitions. Spin splitting of the electron states is due to SIA (a) or BIA (b).

in accordance to Eq. (17). At higher energies, the spectra are determined mainly by the $h1 \rightarrow e1$ and $h2 \rightarrow e1$ transitions. The difference between BIA and SIA spectra is crucial: although in both cases the current for the $h2 \rightarrow e1$ transitions is mainly negative and has a minimum, in the BIA-induced photocurrent these transitions give twice smaller contribution than $h1 \rightarrow e1$, while for SIA-dominance they give the main contribution.

The total circular photocurrent caused by the four kinds of optical transitions is presented in Fig. 3. Arrows in Fig. 3 indicate the points where the transitions start. One can see that the BIA-induced circular photocurrent has a peak in the spectrum, while in the SIA case the dip is present around the same point. This photon energy corresponds to excitation of carriers with $k \approx 2/a$, where a is the quantum well width. At this point the $h1$ and $h2$ energy dispersions have an anti-crossing. This results in a transformation of the hole wave functions and, hence, substantial changes in the dependence $G(k)$ Eq. (14).

The main feature of Fig. 3 is that the BIA-photocurrent has no sign change in the given energy domain, while in the SIA-case it has a sign-variable spectrum. This makes possible to determine the structure symmetry by means of the photogalvanic measurements.

IV. CONCLUDING REMARKS

The situations are possible when the both types of asymmetry are present. The absolute value of the current in the case $\beta_{\text{SIA}} \cdot \beta_{\text{BIA}} \neq 0$ is given by

$$j(\omega) = \sqrt{j_{\text{BIA}}^2(\omega) + j_{\text{SIA}}^2(\omega) \mp 2j_{\text{BIA}}(\omega)j_{\text{SIA}}(\omega) \sin 2\phi}, \quad (18)$$

where ϕ is the angle between \hat{o} and the axis [100]. The upper (lower) sign in Eq. (18) corresponds to $\beta_{\text{BIA}} \cdot \beta_{\text{SIA}} > 0$ (< 0). The direction of the photocurrent is given by the angle χ between [110] and \mathbf{j} :

$$\tan \chi = \frac{j_{\text{SIA}}(\omega) + j_{\text{BIA}}(\omega)}{j_{\text{SIA}}(\omega) - j_{\text{BIA}}(\omega)} \tan(\phi - \pi/4). \quad (19)$$

The angular dependence (18) occurs due to simultaneous presence of Rashba and Dresselhaus fields ($\beta_{\text{SIA}} \cdot \beta_{\text{BIA}} \neq 0$) by analogy with the $\phi_{\mathbf{k}}$ -dependence of the spin splitting. It should be noted that j_{SIA} and j_{BIA} have different excitation spectra that causes complicated ω -dependences of the total photocurrent absolute value and direction, Eqs. (18, 19).

The analysis shows that, under anisotropic scattering, the ‘‘interference’’ terms $\beta_{\text{BIA}} \cdot \beta_{\text{SIA}} / (\beta_{\text{BIA}}^2 + \beta_{\text{SIA}}^2)$ appear in the total photocurrent Eq. (11) even in the linear in β 's regime. This is caused by coupling of the Fourier harmonics of the velocity operator and density matrix in Eq. (6).

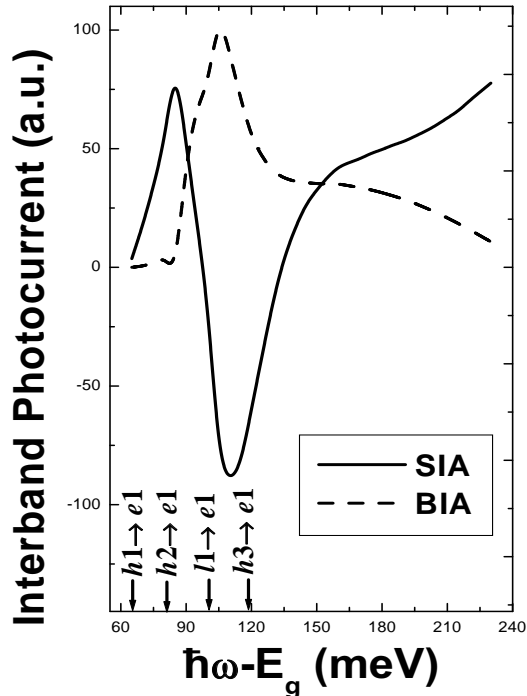


FIG. 3: Spectrum of the interband circular photocurrent due to SIA (solid line) and BIA (dashed line) in a 100-Å wide QW. The arrows indicate the absorption edges for the four optical transitions.

In conclusion, we have developed a theory of the interband circular photogalvanic effect in QWs. The two cases when either BIA or SIA dominates have been considered. It is shown that BIA and SIA result in different photocurrents in QWs. The difference is dramatic at the interband absorption edge, where the photocurrent raises linearly or quadratically with increasing the photon energy under the SIA or BIA dominance, respectively. At higher $\hbar\omega$, the photocurrent excitation spectra also have absolutely different shapes. This makes the interband circular photogalvanic effect a unique high-sensitive tool for investigation of symmetry and spin properties of QWs.

Acknowledgments

Author thanks E.L. Ivchenko for helpful discussions and S.D. Ganichev for critical reading of the manuscript. This work is financially supported by the RFBR, DFG, INTAS, and by the Programmes of Russian Ministry of Science and Presidium of RAS.

* Electronic address: golub@coherent.ioffe.rssi.ru

- ¹ S. A. Wolf, D. D. Awschalom, R. A. Buhrman, J. M. Daughton, S. von Molnár, M. L. Roukes, A. Y. Chtchelkanova, and D. M. Treger, *Science* **294**, 1488 (2001).
- ² S. Datta and B. Das, *Appl. Phys. Lett.* **56**, 665 (1990).
- ³ E. A. de Andrada e Silva, *Phys. Rev. B* **46**, 1921 (1992).
- ⁴ D. Stein, K. von Klitzing, and G. Weimann, *Phys. Rev. Lett.* **51**, 130 (1983).
- ⁵ M.I. D'yakonov and V.Yu. Kachorovskii, *Sov. Phys. Semicond.* **20**, 110 (1986).
- ⁶ B. Jusserand, D. Richards, H. Peric, and B. Etienne, *Phys. Rev. Lett.* **69**, 848 (1992).
- ⁷ P. D. Dresselhaus, C. M. A. Papavassiliou, R. G. Wheeler and R. N. Sacks, *Phys. Rev. Lett.* **68**, 106 (1992).
- ⁸ N.S. Averkiev, L.E. Golub and M. Willander, *J. Phys.: Condens. Matter* **14**, R271 (2002).
- ⁹ E.L. Ivchenko and G.E. Pikus, *Superlattices and Other Heterostructures. Symmetry and Optical Phenomena*, Springer Series in Solid State Sciences, Vol. 110, Springer-Verlag, Heidelberg, 1995; 2nd ed., 1997. Ch. 10.

- ¹⁰ S.D. Ganichev, E.L. Ivchenko, S.N. Danilov, J. Eroms, W. Wegscheider, D. Weiss, and W. Prettl, *Phys. Rev. Lett.* **86**, 4358 (2001).
- ¹¹ S.D. Ganichev, E.L. Ivchenko, V.V. Bel'kov, S.A. Tarasenko, W. Wegscheider, D. Weiss, and W. Prettl, *Nature* **417**, 153 (2002).
- ¹² I.A. Merkulov, V.I. Perel', and M.E. Portnoi, *Sov. Phys. JETP* **72**, 669 (1991).
- ¹³ Expressions for the real coefficients N , W_{\pm} , ζ , Q_{\pm} , and for the functions $C(z)$ and $S(z)$ are given in Ref. 12 in the approximation of infinitely-high barriers.
- ¹⁴ E.L. Ivchenko, Yu.B. Lyanda-Geller and G.E. Pikus, *Sov. Phys. JETP* **71**, 550 (1990).
- ¹⁵ The contribution of the only allowed transition $l1 \rightarrow e1$ is proportional to $(\tau_h - \tau_e)$ at $k = 0$, therefore we take different values for τ_e and τ_h in order to obtain a step-like behaviour of the spectrum. It is clearly seen in the corresponding curves in Figs. 2a and 2b.